INTERFACE

royalsocietypublishing.org/rsif

Research

Cite this article: Wei N, Xiong X, Li Q, Feng M, Szolnoki A. 2026 Cooperation in public goods games over uniform random hypergraphs with game transitions. *J. R. Soc. Interface* **23**: 20251319.
https://doi.org/10.1098/rsif.2025.1319

Received: 17 December 2025
Accepted: 9 April 2026

Subject Category:
Life Sciences – Physics interface

Subject Areas:
computational biology, evolution

Keywords:
uniform random hypergraph, public goods game, game transition, group cooperation dynamics

Authors for correspondence:
Qin Li
e-mail: qinli1022@swu.edu.cn
Minyu Feng
e-mail: myfeng@swu.edu.cn

Supplementary material is available online at https://doi.org/10.6084/m9.figshare.c.8439809.

THE ROYAL SOCIETY PUBLISHING

Cooperation in public goods games over uniform random hypergraphs with game transitions

Nankun Wei[1], Xiaojin Xiong[1], Qin Li[2], Minyu Feng[1] and Attila Szolnoki[3]

[1]College of Artificial Intelligence and [2]Business College, Southwest University, Chongqing, People's Republic of China
[3]Institute of Technical Physics and Materials Science, Centre for Energy Research, Budapest, Hungary

NW, 0009-0007-0474-5906; XX, 0009-0009-5601-7833; QL, 0000-0001-5480-0992; MF, 0000-0001-6772-3017; AS, 0000-0002-0907-0406

The evolution of cooperation is a central enigma in evolutionary game theory. Traditionally, the combination of pairwise networks and repeated public goods games (PGGs) with a single state fails to adequately describe realistic group interaction scenarios. On the one hand, pairwise networks lack clear group definitions. On the other hand, a participant's decision affects not only competitors' fitness but also the state of the surrounding environment. To address this problem, we propose a PGG with game transition mechanisms based on uniform random hypergraphs (URH). In our model, game groups formed by hyperedges transition between two types of games, one with abundant public resources and the other with scarce public resources. The transition probability is closely related to the strategies of players within the hyperedges. By developing a Monte Carlo simulation framework that incorporates payoff accumulation, strategy imitation and game state transitions, we aim to reveal the co-evolutionary patterns of strategies and game states in group interactions. Our study highlights a nonlinear relationship between defection sensitivity and cooperation frequency under game transitions, as well as the asymmetric effects of the two sensitivities in state-dependent transitions. These observations open new directions for approaching social dilemmas.

1. Introduction

Cooperative behaviours are prevalent in both natural and social systems and have attracted extensive scholarly attention [1,2]. From teamwork and resource sharing in human societies to the collaborative scheduling of distributed energy nodes in smart grids, cooperative interactions among individuals play an indispensable role. However, when individuals face the dilemma between 'personal gain' and 'collective benefit', rational choices often favour defection. This makes the emergence and maintenance of group cooperation in social dilemmas a pressing scientific challenge [3,4]. Evolutionary game theory provides a robust theoretical foundation and an effective framework for studying this phenomenon. Within this framework, game models, such as the prisoner's dilemma [5–7], donation game [8], snowdrift game [9,10] and public goods game (PGG) [11,12], have been extensively studied.

As a classic multiplayer game model, the PGG reveals the fundamental logic of social dilemmas: rational defection by participants leads to the tragedy of the commons [13], while mutual cooperation among individuals yields higher collective benefits [14,15]. To investigate the factors influencing cooperative behaviours in PGG, researchers have thoroughly explored various mechanisms, such as rewards [16], punishments [17], heterogeneity [18,19],

reputation [20], memory [21–23] and strategy persistence [24]. Many of these investigations into mechanisms are conducted under the spatial structure characterized by pairwise networks, because depicting real-world group interactions requires not only well-defined interaction rules but also a clear spatial structure as the underlying carrier. Some studies have systematically summarized the differences in cooperative dynamics of PGG across classical pairwise networks (including regular lattices, heterogeneous scale-free networks and small-world networks) [25]. Nevertheless, a fundamental limitation of pairwise networks as the carrier for group interactions is their failure to provide a rigorous and unambiguous definition of groups [26]. In supplementary material, fig. S1, specific examples are used to illustrate that ambiguous group definitions directly lead to a series of issues in game interactions.

Furthermore, the environments of group games in the real world are not static. Consequently, in recent years, the academic community has grown increasingly interested in the co-evolutionary dynamics of strategies and environments [27–29]. When individual strategies not only influence immediate payoffs but also reshape subsequent game types through resource allocation or group dynamics, the so-called 'game transitions' occur [30]. Addressing this phenomenon, Su *et al.* [31] found that dynamic switching between game states of varying dilemma strength can lower the critical threshold for the evolution of cooperation, while Feng *et al.* [32] demonstrated that Markov-based game-state transitions can reinforce cooperation through psychological effects. However, existing studies on multiplayer game transition models under spatial structures are all built on traditional pairwise networks. The ambiguous group definitions of pairwise networks may result in individuals without direct connections being placed in the same group in multiplayer game scenarios, thereby exerting unrealistic effects on each other's payoffs.

In recent years, higher-order interaction models, particularly hypergraphs and simplicial complexes, have offered new insights for addressing these challenges [33–36]. Hypergraphs directly connect multiple nodes through hyperedges, naturally embodying the group characteristic of all individuals within a group being interconnected, and can provide clear group definitions. They have been applied to scenarios, such as PGG and collective intelligent interactions. Alvarez-Rodriguez *et al.* [26] systematically proposed algorithms for constructing uniform random hypergraphs (URH) and heterogeneous hypergraphs, with results indicating that higher-order interactions can significantly enhance cooperation stability. Building on this foundation, some studies [37,38] found that heterogeneous investments effectively promote cooperation across hypergraphs of different orders. Civilini *et al.* [39] explored the differences in collective behaviour dynamics between traditional graphs and hypergraphs, revealing that compared with pairwise interactions, higher-order interactions not only foster cooperation in competitive environments but also trigger explosive cooperative behaviours. Battiston *et al.* [40] further emphasized that higher-order structures capture group-level dynamics invisible in pairwise models, shedding light on mechanisms of cooperation and collective behaviour in human systems. In addition, Shi *et al.* [41] applied hypergraphs to multi-agent Q-learning dynamics, establishing a theoretical framework based on URH. Zou & Huang [42] also examined the effect of punishment on cooperative dynamics in hypergraphs. These studies demonstrate that hypergraphs provide a more suitable spatial structure for investigating the emergence of cooperation under group interactions, and their clear group definitions ensure that each group is equivalent to a complete subgraph—perfectly addressing the aforementioned shortcomings of pairwise networks in supporting multiplayer games and game transitions.

By building on these observations, we here propose a PGG model with transition mechanisms based on URH. In particular, we use hyperedges as fundamental game units, with each hyperedge corresponding to a PGG group. In response to varying environmental conditions, the model distinguishes between high-value and low-value game states based on differences in synergy factors. Specifically, high-value games correspond to a higher synergy factor than low-value games, which in turn naturally results in a lower degree of social dilemma for the former. The transition probabilities of hyperedges are determined by the proportion of cooperators within the group, with sensitivity coefficients regulating the responsiveness of different states to defection. This design preserves the advantages of hypergraphs in modelling higher-order interactions while enabling dynamic feedback from collective environments to individual behaviours. Through systematic Monte Carlo simulations, we reveal cooperation dynamics and formation mechanisms in group settings, offering new insights into understanding and sustaining cooperation in real-world social dilemmas.

The paper is organized as follows: §2 details the interaction system and specific rules for payoff accumulation, strategy learning and game transitions. Section 3 presents the effects of different parameters on system cooperation dynamics, accompanied by analysis. Finally, §4 summarizes the cooperation dynamics observed in the model and outlines future research directions.

2. Model

High-order interactions are prevalent in real-world group settings, and individual behaviours shape not only their own and their partners' outcomes but also the group environment. For example, overgrazing brings short-term gains to individuals but depletes public resources, undermining long-term benefits. To model how individual actions affect payoffs and the environment, we develop a group-interaction system based on URH. Here, agents engage in repeated PGG via hyperedges, updating their strategies while their choices influence the game states of the hyperedges they belong to. This section outlines the model's core set-up: URH construction, strategy update rules and game transition mechanisms.

2.1. Interaction network

In the framework of hypergraphs, a hypergraph is denoted as $H(N, L)$, where $N = \{n_1, n_2, \ldots, n_{|N|}\}$ represents a set of n nodes, each node corresponds to an agent, and $L = \{l_1, \ldots, l_m\}$ represents a set of m hyperedges, each hyperedge corresponds to a group

where PGG take place. Each hyperedge can contain two or more agents, and an agent may belong to multiple different hyperedges simultaneously. Thus, the hyperdegree k_i is used to characterize the number of hyperedges to which agent i belongs.

Our model focuses on the overall dynamics exhibited by the system through agent interactions. We assume that each agent has equal status and is indistinguishable from one another, i.e. our interaction system is homogeneous and uniform. Therefore, we use URH [26] for characterizing the interaction relationships among agents in the system.

For a URH with N nodes, each node is assigned to a hyperedge with equal probability, and each hyperedge contains exactly g nodes. Such a uniform hypergraph is termed a g-order uniform hypergraph, and there exists a critical threshold for the number of hyperlinks $L_c = (N/g) \ln N$ [26] to ensure that the hypergraph is fully connected.

2.2. Strategy update

Based on the agent interaction system characterized by URH, we allow agents to participate in PGG with hyperedges as groups. Let s_i denote the strategy adopted by agent i, which can take two values: 0 represents defection (D), and 1 represents cooperation (C). Here, we take the payoff calculation of agent i as an example to demonstrate the specific payoff calculation process and the strategy update rules.

A random agent i and one of its hyperedges l are selected, and all agents in l participate in PGG across all their respective hyperedges and accumulate their payoffs. First, we define the payoff of node i in hyperedge l as $\pi_{i,l}$, which is calculated as

$$\pi_{i,l} = r_l \cdot \sum_{u \in l} c \cdot s_u - c \cdot s_i, \tag{2.1}$$

where the cooperation cost c is fixed at 1, and $\sum_{u \in l} c \cdot s_u$ is the total contribution of cooperators in l. Here, $r_l = R_l/g$ is the normalized synergy factor, where R_l is the raw synergy factor and g is the size of hyperedge l. The total contribution is multiplied by r_l, and agent i pays the cooperation cost c according to its current strategy.

We define the final payoff of agent i as

$$\pi_i = \frac{1}{k_i} \sum_{l' \in \Omega_i} \pi_{i,l'}, \tag{2.2}$$

where Ω_i denotes the set of all hyperedges containing agent i. Agent i is required to participate in games and accumulate payoffs across these hyperedges; k_i represents the hyperdegree of agent i, i.e. the number of hyperedges to which it belongs, and is used to average the total payoff.

By analogy, after all agents in l have accumulated their payoffs, the highest earner j in hyperedge l is identified, and agent i imitates the strategy of j with probability $W_{s_i \to s_j}$ defined as

$$W_{s_i \to s_j} = \frac{1}{\Delta} \left[\pi_j - \pi_i \right]. \tag{2.3}$$

This linear imitation mechanism is a commonly used strong selection rule in higher-order interaction game studies [26,37]. In the formula, $\pi_j - \pi_i$ represents the payoff difference between the two agents. Since j is the agent with the highest payoff in hyperedge l, this payoff difference is non-negative; Δ represents the absolute value of the maximum possible payoff difference in the current system, which is used to ensure the normalization of the imitation probability. We use superscripts for differentiation: π_D^+ denotes the maximum possible payoff for defectors, and π_D^- refers to the minimum possible payoff. The notation for cooperators adheres to the same convention. Thus, the maximum and minimum payoffs for different strategies are calculated as

$$\begin{cases} \pi_D^+ = r_1(g-1), \\ \pi_D^- = 0, \\ \pi_C^+ = r_1 g - 1, \\ \pi_C^- = r_2 - 1, \end{cases} \tag{2.4}$$

where r_1 and r_2 represent two values of the normalized synergy factor, and their specific meanings are elaborated in §2.3. From this, Δ has four possible value combinations. Given $r_2 \le r_1$, the calculation formula of Δ under different value ranges of r_1 and r_2 is derived by comparison

$$\Delta = \begin{cases} r_1(g-1) - (r_2 - 1), & 0 < r_2 < r_1 < 1, \\ r_1 g - r_2, & 0 < r_2 \le 1 \le r_1, \\ r_1 g - 1, & 1 < r_2 < r_1. \end{cases} \tag{2.5}$$

To facilitate understanding of the strategy imitation process, we present a partial network schematic in figure 1. Agents are represented as nodes, with their strategies distinguished by different colours. The strategy imitation process is probabilistic. In the strategy imitation stage, we take defector agent i as an example, demonstrating a typical scenario where it successfully learns the strategy of agent j, the highest earner in the hyperedge, and ultimately switches to cooperation.

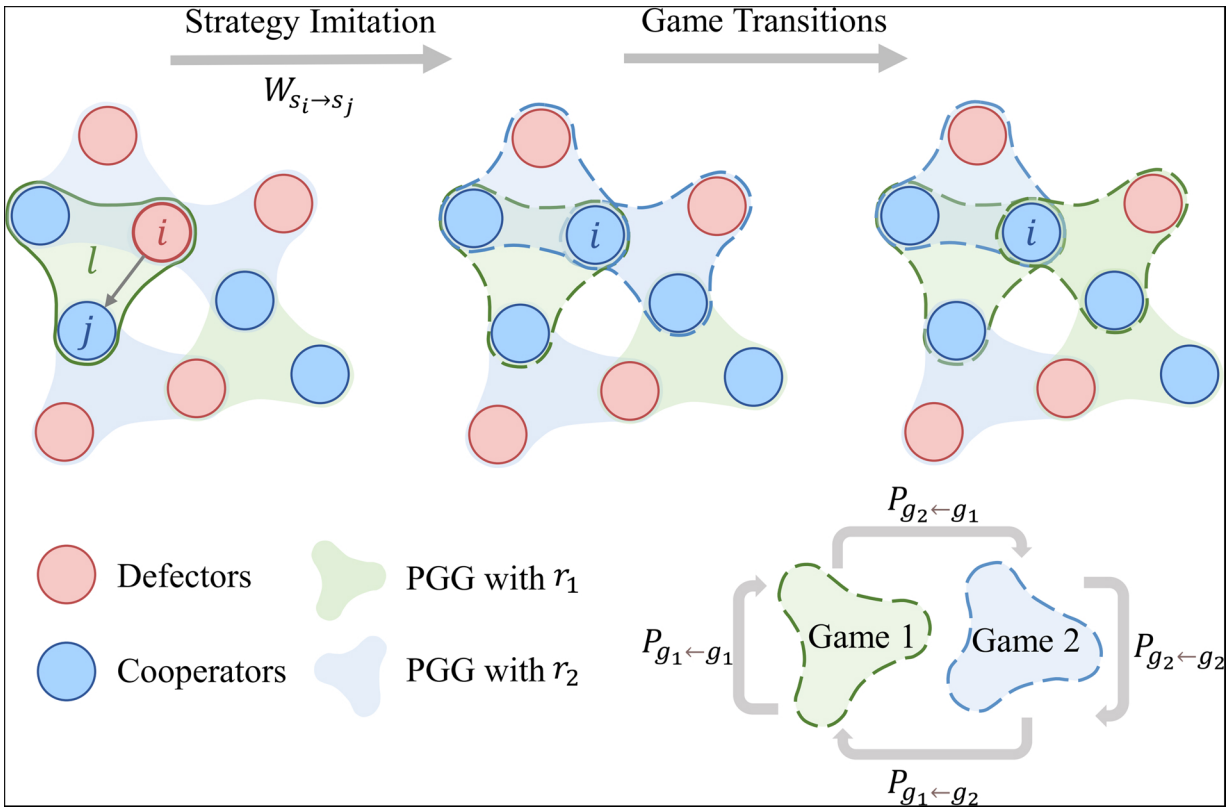

Figure 1. Strategy update and game transition process. Nodes represent agents. Blue nodes are cooperators and red nodes are defectors. Hyperedge colours correspond to game states. Green hyperedges indicate high-value game g_1 with r_1 and blue hyperedges indicate low-value game g_2 with r_2, and $r_1 > r_2$. The dynamics contains two steps. **(a) Strategy imitation:** an agent i is selected randomly and one of its hyperedges l (solid border) is chosen randomly. Agents in l accumulate payoffs based on the current game state. Agent i then imitates the strategy of the highest earning agent j in l with probability $W_{s_i \to s_j}$. **(b) Game transition:** following the strategy update step for player i, regardless of whether its strategy is changed or not, all hyperedges containing i (dashed borders) undergo transitions. These transitions rely on their cooperator fractions and follow the rules at the bottom right. Cooperation promotes transitions to g_1 while defection leads to g_2. These two transitions alter payoff structures and produce distinct cooperation dynamics compared to single PGG.

2.3. Game transition

The core idea of game transitions is that players' strategies not only affect current payoffs but also influence subsequent game types. A classic and realistic assumption is that cooperative behaviours improve the game environment, while defection deteriorates it. Therefore, cooperative behaviours increase the probability of transitioning to the high-value game system, while defection increases the probability of transitioning to the low-value system.

To avoid conceptual confusion, it is necessary to clarify the distinction between our game transition mechanism and reputation mechanism (e.g. the LR2 reputation mechanism [43]). Reputation focuses on interactions and evaluations among individuals, whereas the game transition mechanism centres on the reciprocal influence between individual strategies and the environment. These two mechanisms target different objects of interaction but are not mutually conflicting.

Our research focus is not on designing or calculating transition probabilities between multiple game states. Instead, we prioritize the cooperative dynamics exhibited by the co-evolution of strategies and the environment in higher-order spatial structures, thereby adopting a two-state game transition framework. Given the structural characteristics of hypergraphs, we assume that each hyperedge l has a unique synergy factor that takes only two possible values: r_1 or r_2 (with $r_2 \leq r_1$). Specifically, r_1 corresponds to a state of abundant environmental resources, where a relatively mild social dilemma exists, and players can obtain significant payoffs through cooperation, thus corresponding to high-value games. In contrast, r_2 corresponds to a state of scarce environmental resources, where the efficiency of public resource enhancement is low. Even if individuals choose to cooperate, they struggle to overcome the payoff bottleneck owing to the more severe social dilemma, making such games low-value ones. To intuitively reflect the resource advantage of the high-value game relative to the low-value game and simplify subsequent descriptions, we define $\delta = r_1 - r_2$.

Based on this, all interaction groups in the system are divided into two subsystems: the high-value game subsystem g_1 and the low-value game subsystem g_2. Under the transition mechanism, there are corresponding state transition probabilities between these two subsystems.

Taking hyperedge l as an example, equations (2.6) and (2.7) show the probabilities of transitioning into the high-value game when hyperedge l is in different game states, while $P_{g_2 \leftarrow g_1} = 1 - P_{g_1 \leftarrow g_1}$ and $P_{g_2 \leftarrow g_2} = 1 - P_{g_1 \leftarrow g_2}$ represent the probabilities of

transitioning into the low-value game, including

$$P_{g_1 \leftarrow g_1} = \left(\frac{\sum_{u \in l} s_u}{g} \right)^{\alpha_1} \tag{2.6}$$

and

$$P_{g_1 \leftarrow g_2} = \left(\frac{\sum_{u \in l} s_u}{g} \right)^{\alpha_2}. \tag{2.7}$$

Here, $\frac{\sum_{u \in l} s_u}{g}$ denotes the proportion of cooperators within hyperedge l, with the basic transition probability directly determined by this proportion. This setting conforms to the classical framework of coevolution between the game environment and agents' strategies during game transitions [30,31], in which cooperation enhances the game environment while defection degrades it. Building on this proportion of cooperators, we incorporate exponential sensitivity coefficients α_1 and α_2 to adjust the basic probability. This design is widely utilized in co-evolutionary mechanism research [24,37] as exponential sensitivity avoids the uniform environmental response to strategy changes inherent in linear functions, enabling the characterization of varied environmental sensitivity to defection. Specifically, α_1 and α_2 regulate the sensitivity of hyperedges to defection across different subsystems and define the nature of game transitions. In the context of subsystem transitions, a transition is state-independent if its probability depends exclusively on the target subsystem's characteristics rather than the current subsystem. Conversely, it is state-dependent if the probability of transitioning to the same target subsystem differs based on the current subsystem.

First, we consider the case where $\alpha_1 = \alpha_2$. In this case, the state transition has no memory effect. The transition probability is independent of the current and past states of the hyperedge, i.e. the game transition is state-independent. To simplify, we denote $\alpha_1 = \alpha_2 = \alpha$. When $\alpha = 0$, the entire system degenerates back to a single PGG of pure g_1, and the game type of the hyperedge does not respond to the players' defection behaviours. Suppose that the value of α gradually increases. In that case, the environment in the system becomes more sensitive to the defection of agents, and a hyperedge can only transition to the high-value game system with a high probability when the number of defectors in it is very small.

Next, we consider the case where $\alpha_1 \neq \alpha_2$. In this case, the game transition is state-dependent. Such transitions satisfy the Markov property, the transition probability at the next step depends only on the current state, and is independent of the past states of the hyperedge [30]. When $\alpha_1 < \alpha_2$, the hyperedges in g_1 are less sensitive to defection than those in g_2. If two hyperedges have the same number of cooperators, the hyperedge in the g_1 state is more likely to remain in g_1 in the future, while the hyperedge in the g_2 state is more difficult to transition into g_1, vice versa when $\alpha_1 > \alpha_2$.

In figure 1, we continue to focus on agent i and explain the effect of its strategy change on the hyperedges to which it belongs. Note that only one possible transition outcome is shown in the figure, so the state dependence of transition probabilities is not reflected. Specifically, the transition results of the three hyperedges marked by dashed lines in the figure are as follows: the hyperedge composed entirely of cooperators will remain in the high-value game state with a probability of 1. Among the other two hyperedges, one stays in the low-value game state represented by blue, and the other successfully transitions to the high-value game state and turns green.

3. Simulation and analysis

This section investigates the cooperation dynamics of PGG with transition mechanisms on URH through Monte Carlo simulations. We analyse the system by extending game transitions from state-independent to state-dependent scenarios and by employing asynchronous random sequential updating.

The system is uniformly initialized with equal proportions. Agents are randomly assigned to either cooperation or defection, each accounting for 50%. Similarly, hyperedges are randomly initialized to either high-value (g_1) or low-value (g_2) game states, each accounting for 50%. To ensure the reliability of the results, we verify the robustness of the data across different initialization ratios of cooperators and hyperedge states; detailed analyses are provided in supplementary material, §S2.

One Monte Carlo step consists of N elementary steps. In each elementary step, a target node and one of its affiliated hyperedges are selected. Subsequently, payoffs for all players in the target hyperedge are accumulated, the target node's strategy is updated and game transitions are performed for all hyperedges containing the target node. To ensure stable results, we construct a URH with $|N| = 1000$ and $|L| = L_c$, set the iteration steps to $T = 10^4$ and use data from the last 4000 steps for averaging under different parameter combinations. To ensure the stability of the numerical results, we calculated the average of the critical value data points using data from at least 30 independent simulations.

3.1. State-independent transitions

Unlike traditional single-game scenarios, the transition mechanism enables hyperedges to switch between high-value (g_1) and low-value (g_2) game states. A natural question is whether the overall dynamics exhibited by the system represents a simple superposition of the cooperative dynamics of these two individual game states.

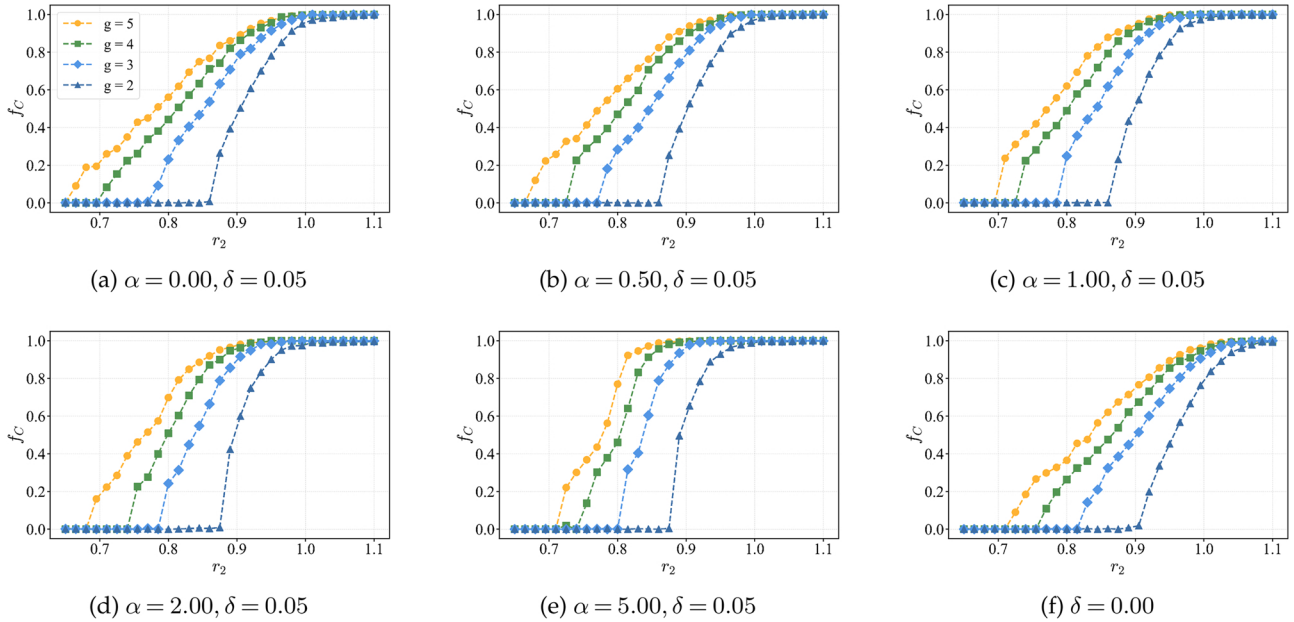

Figure 2. Cooperation frequency f_C as a function of r_2 under different sensitivity levels. The x-axis represents the low-value synergy factor r_2, with curves for different hypergraph orders: yellow circles ($g = 5$), green squares ($g = 4$), blue diamonds ($g = 3$) and purple triangles ($g = 2$). Panels (a)–(e) set $\delta = 0.05$ with $\alpha = 0, 0.5, 1, 2, 5$, respectively. Panel (f) shows the single low-value game without game transitions ($\delta = 0$). From panels (a)–(e), as the system's sensitivity to defection increases, this transition mechanism raises the cooperation threshold while amplifying f_C growth to boost cooperation for high r_2. This compresses the r_2 interval required for f_C to rise from 0 to 1, leading to a steeper curve trend.

To verify this conjecture, we first set $\delta = r_1 - r_2 = 0.05$ to ensure a moderate difference between the two game states. We then examine how the cooperation frequency f_C varies with the low-value synergy factor r_2 under different sensitivity levels α; the results are shown in figure 2.

Figure 2 first illustrates how the cooperation frequency associated with the sensitivity coefficient α behaves across the pairwise and higher-order interactions characterized by the URH, under the state-independent condition $\alpha_1 = \alpha_2 = \alpha$. We define the critical value r_{2c} as the minimum r_2 required to sustain cooperation. Overall, as the interaction order g increases, the critical r_{2c} for higher-order interactions ($g > 2$) to maintain cooperation is significantly lower than that for pairwise interactions ($g = 2$). This result aligns with findings reported in [26] and [39].

The sensitivity coefficient α quantifies a hyperedge's sensitivity to defection, and its regulatory effect on cooperation shows a nonlinear trend with the increase of r_2. Specifically, for the cooperation extinction threshold r_{2c}, a higher α elevates the r_{2c} threshold more markedly, indicating that increased defection sensitivity suppresses cooperation under strong social dilemmas in g_2.

In contrast, as r_2 increases, that is, as the social dilemma intensity in the low-value game g_2 weakens, the cooperation-promoting effect of the transition mechanism gradually emerges. A higher sensitivity coefficient α significantly boosts the cooperation frequency, and this promoting effect is more pronounced in higher-order interactions.

This is because pairwise interactions involve small groups and have low tolerance for defection. Even if the social dilemma is alleviated, a group can switch to the high-value game only when both individuals cooperate. In contrast, higher-order interactions tolerate defection better. For example, when a group has only one defector, a five-player group ($g = 5$) has a much higher probability of switching to the high-value game than a pairwise group. To verify the universality of the URH, we additionally conduct comparative simulations on the *Erdős–Rényi* random network to characterize pure pairwise interaction scenarios. The results (supplementary material, fig. S2) demonstrate that the URH can not only accommodate the characterization of higher-order interactions through flexible adjustment of the interaction order g but also accurately describe pairwise interactions when $g = 2$. In addition, to validate the robustness of our conclusions, we conduct supplementary simulations on randomly connected mixed-order hypergraphs (supplementary material, §S3). Results confirm that our core findings remain consistent under mixed-order structures: cooperation is still significantly promoted as the average interaction order increases.

These further support the core conclusion on the URH. Higher-order interactions promote cooperation more effectively than pairwise interactions. Under the transition mechanism, the nonlinear influence of the defection sensitivity coefficient α on f_C is more significant in higher-order interactions.

With the variation of r_2, we find that the law of how this nonlinear effect is regulated by the intensity of the social dilemma in low-value games (g_2) is as follows: in scenarios with a strong social dilemma (small r_2), cooperative strategies are hard to sustain owing to the conflict between individual rationality and collective interests. Increasing defection sensitivity further tightens the criteria for game state transitions, making the already fragile cooperative system less resistant to defection and raising the threshold r_{2c} for sustaining cooperation. In contrast, in scenarios with a weak social dilemma (large r_2), cooperation already forms a preliminary group foundation. Increasing defection sensitivity at this stage incentivizes cooperative behaviour, because

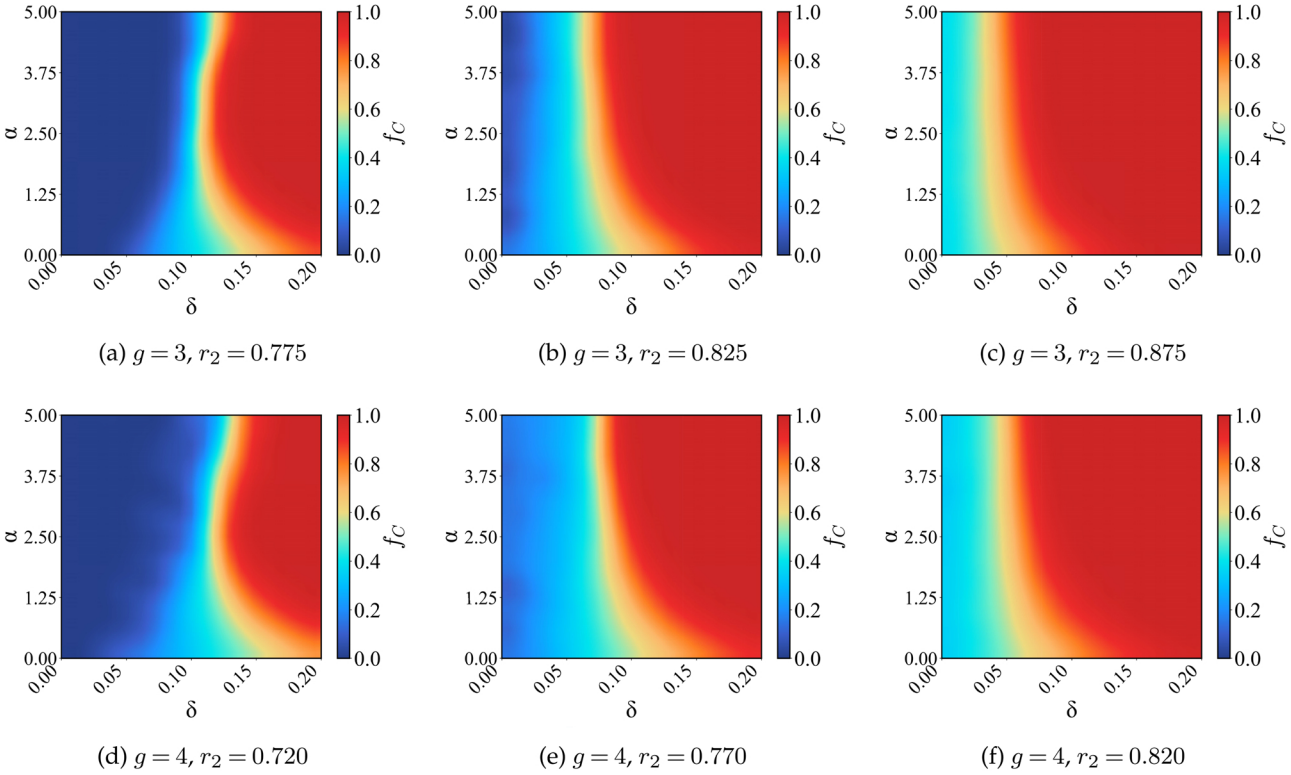

Figure 3. Heatmaps of cooperation frequency f_C as functions of δ and α for representative r_2 values. The first row corresponds to $g = 3$ with $r_2 = 0.775, 0.825, 0.875$. The second row corresponds to $g = 4$ with $r_2 = 0.72, 0.77, 0.82$. Heatmaps are mildly smoothed with a Gaussian filter ($\sigma = 1$) to suppress numerical fluctuations, and bilinear interpolation is used for visualization. At the boundaries between pure cooperation and pure defection for different hypergraph orders, three consistent phenomena are observed as the sensitivity α increases: cooperation is inhibited, the cooperation level remains stable and cooperation is promoted.

cooperator clusters are more likely to switch to the high-value game g_1 and gain higher payoffs, thereby attracting more individuals to cooperate and leading to a sustained rise in the cooperation frequency f_C.

To further explore the nonlinear effect of defection sensitivity α on f_C under higher-order interactions, we select three representative values of r_2 for each system with $g = 3$ and $g = 4$, corresponding to three levels of social dilemma intensity in single low-value games g_2: unsustainable cooperation, barely sustainable cooperation and stably sustainable cooperation. Heatmaps are used to visualize the joint effects of defection sensitivity α and the relative resource advantage of high-value games $\delta = r_1 - r_2$ on f_C; the results are shown in figure 3.

In the strong social dilemma scenario shown in figure 3*a*,*d*, the phase diagrams exhibit distinct pure-defection regions. This indicates that the system's cooperation frequency f_C depends entirely on the high-value game g_1, and can only be sustained when the resource advantage $\delta = r_1 - r_2$ is sufficiently large. As the defection sensitivity coefficient α, which quantifies how responsive hyperedges are to defection, increases, the boundary between the pure-defection and mixed cooperation-defection regions shifts rightward, making it harder for cooperation to persist when g_1 has only a small resource advantage (small δ).

In the moderate social dilemma scenario shown in figure 3*b*,*e*, no pure defection regions are observed; this is because the low-value game g_2 alone can barely sustain cooperation when there is no resource advantage ($\delta = 0$). A moderate increase in the defection sensitivity coefficient α shifts the pure-cooperation regions to the left, expanding the range of δ values that support full cooperation.

In the weak social dilemma scenario shown in figure 3*c*,*f*, this pattern is further validated, and an appropriate increase in the defection sensitivity coefficient α directly boosts the system's overall cooperation frequency f_C.

Overall, when the intensities of the social dilemma in both game states are adjusted simultaneously, the nonlinear influence of the defection sensitivity coefficient α on the cooperation frequency f_C can be categorized into three types of cooperative dynamics. As α increases, f_C exhibits full extinction (dropping to 0), stable maintenance (remaining nearly unchanged) or positive feedback growth (rising continuously).

The specific cooperative dynamics depend on the ability of g_2 to sustain cooperation independently and the resource advantage δ of g_1. When the low-value game g_2 corresponds to a strong social dilemma, it cannot sustain cooperation on its own. A high defection sensitivity α suppresses cooperation unless the high-value game g_1 provides a large resource advantage δ. When g_2 corresponds to a weak social dilemma, it can sustain cooperation independently. As α increases, the region of full cooperation expands, even if the resource advantage δ of g_1 is small.

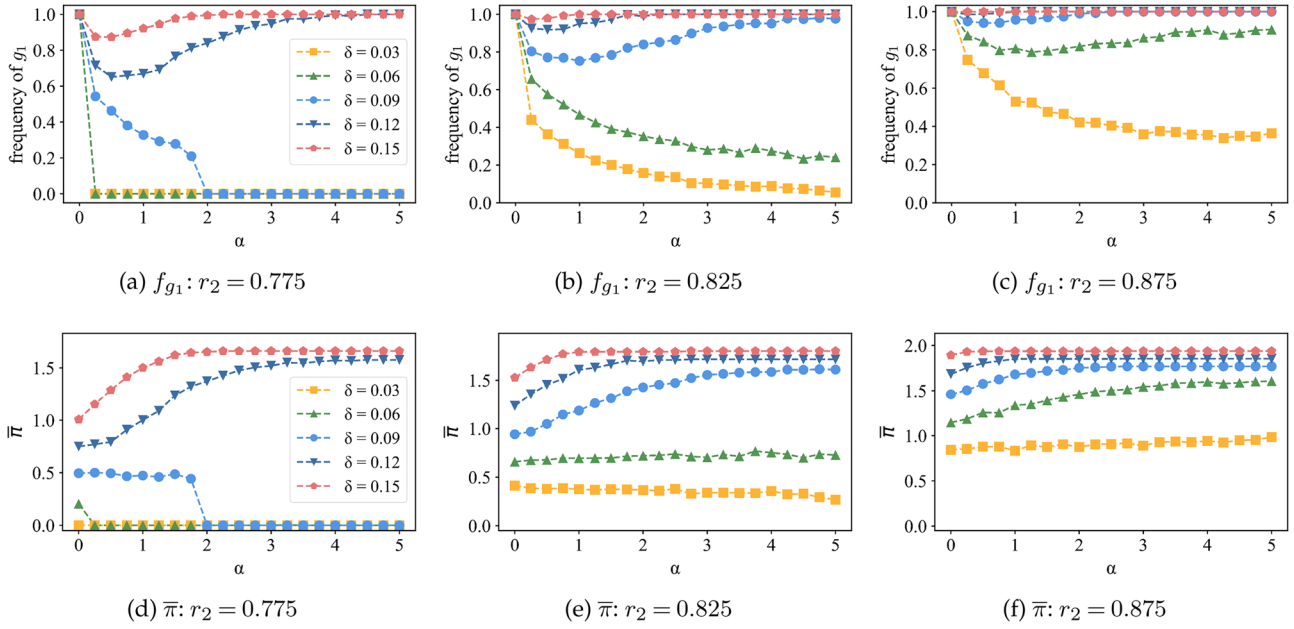

Figure 4. f_{g_1} and $\overline{\pi}$ dependence of α for three representative r_2 values. We fix $g = 3$ for all panels while the different values of δ are indicated in the legend. Left, middle and right columns show low, intermediate and high r_2 values, which are 0.775, 0.825 and 0.875, respectively. In each column, panels exhibit cooperative positive feedback when δ is large. For small δ, in the first column, g_2 cannot sustain cooperation independently, causing f_{g_1} and $\overline{\pi}$ to decline to 0. In other panels, f_{g_1} decreases but remains non-zero, while $\overline{\pi}$ stays stable.

To investigate the cause of this nonlinearity, we define L_{g_1} as the number of g_1 hyperedges, where $f_{g_1} = L_{g_1}/L_c$ represents the proportion of g_1 in the system. This proportion is crucial for cooperation maintenance and positive feedback. For $g = 3$, we select the same three r_2 values as in figure 3 to represent three levels of social dilemmas with different intensities in the low-value game. Across these three levels of social dilemma intensity, we separately explore how the relative resource advantage δ of the high-value game g_1 affects variations in f_{g_1} and the average payoff $\overline{\pi}$, with the results shown in figure 4.

Figure 4 shows that positive feedback emerges across all r_2 scenarios, with the fraction of high-value games f_{g_1} initially decreasing and then recovering. This occurs because a larger α enhances the cooperation purity of hyperedges in g_1. While f_{g_1} declines, the cooperation quality of hyperedges in g_1 increases. Cooperative clusters face a lower risk of exploitation by defectors and possess an intrinsic resource advantage, thereby gaining an increasingly strong payoff advantage. This drives a continuous rise in global cooperation, which further leads to the rebound of f_{g_1}.

The corresponding average payoff curve maintains an upward trend; this confirms that g_1 can sustain a payoff advantage for cooperators. Concurrently, the system's social welfare is reflected in the average payoff of agents [44]. This upward payoff trend demonstrates that the promotion of cooperation is accompanied by a synchronous increase in social welfare. Notably, figure 4*a* reveals that even when the low-value game g_2 is in a strong social dilemma, the system can still trigger positive feedback if the resource advantage δ of the high-value game g_1 is significant enough to provide an adequate payoff advantage for cooperation.

Conversely, when δ is small, the high-value game cannot sustain a payoff advantage for cooperation. The average payoff does not increase with the rise of defection sensitivity α, and the proportion of high-value games f_{g_1} decreases monotonically. At this point, the cooperative support capacity of the low-value game determines whether the system's cooperation persist or goes extinct. In figure 4*a*, when the low-value game g_2 cannot sustain cooperation on its own, the system evolves entirely into the low-value game as α increases, ultimately leading to the collapse of cooperation. Correspondingly, figure 4*d* demonstrates that social welfare decays to zero as cooperation collapses. In contrast, figure 4*b*,*c* shows that when the social dilemma of the low-value game g_2 is alleviated and it possesses cooperative support capacity, naturally formed cooperator clusters can stabilize g_1 at a non-zero level. At this point, social welfare also maintains a relatively stable trend.

This further explains how the two game states give rise to the three cooperative dynamics shown in figure 3. Cooperation can form positive feedback only when the high-value game g_1 provides a significant resource and payoff advantage. If g_1 fails to maintain such an advantage for cooperative behaviour, then the independent ability of the low-value game g_2 to sustain cooperation determines whether the system reaches stable cooperation or collapses into full defection. Furthermore, the numerical results demonstrate a notable positive correlation between cooperative behaviour and social welfare under the game transition mechanism. The promotion of cooperative actions enhances social welfare, while their inhibition leads to reduced social welfare.

3.2. State-dependent transitions

Finally, we consider state-dependent transition probabilities, where hyperedges in different game states exhibit varying sensitivities to defection by agents within the edges.

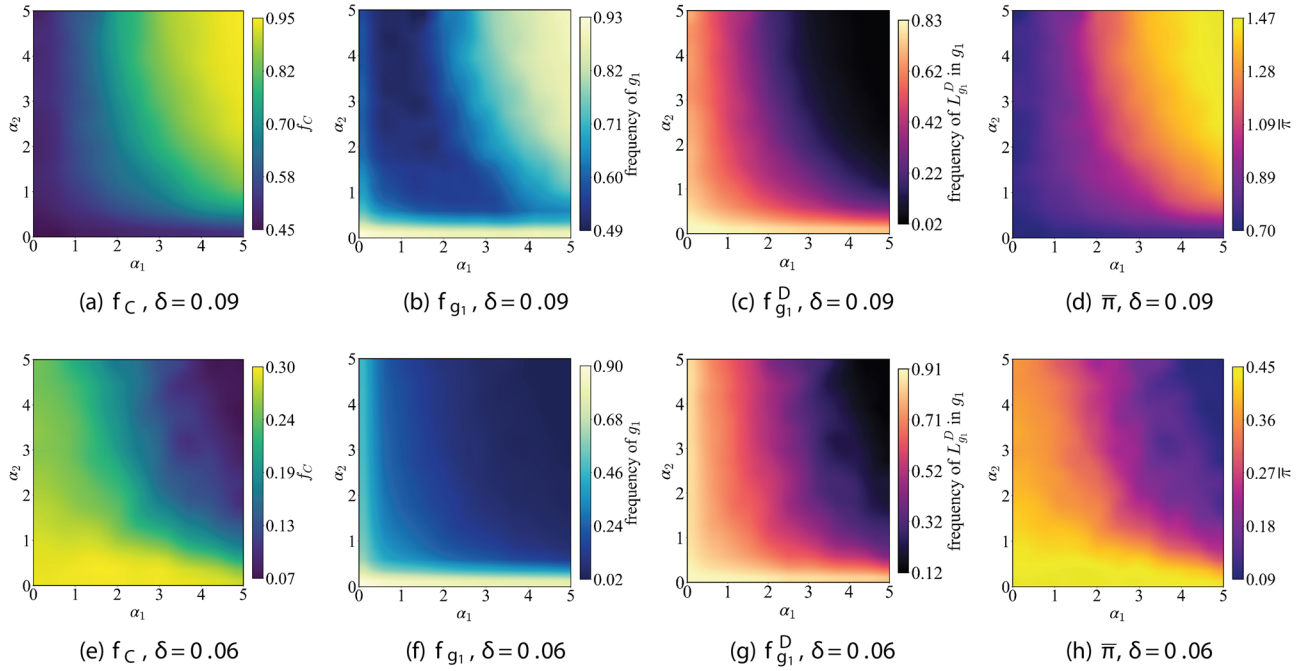

Figure 5. Heatmaps of metrics under different δ values. Left to right in each row, panels show cooperation frequency f_C, g_1 proportion f_{g_1}, defector-containing hyperedges $f^D_{g_1}$ and average payoff $\overline{\pi}$, respectively. Heatmaps are mildly smoothed with a Gaussian filter ($\sigma = 1$) to reduce numerical noise, and bilinear interpolation is used for visualization clarity. The first row corresponds to the changes in various indicators when cooperation forms positive feedback, while the second row depicts the scenario where cooperation goes extinct as sensitivity increases. Results in the first column directly demonstrate the asymmetric variation of f_C with α_1 and α_2 under the state-dependent game transition scenario, and analyses of other indicators also exhibit a similar asymmetric phenomenon.

From previous analyses, when g_2 cannot sustain cooperation independently, the g_1 subsystem becomes critical for maintaining cooperation and even fostering positive feedback in the entire system under the transition mechanism. We characterize the importance of g_1 to system-wide cooperation using two metrics. The first is f_{g_1}, the proportion of g_1 hyperedges in the entire system as previously defined. The second is $f^D_{g_1}$, the fraction of hyperedges in g_1 that contain defectors (D). It is defined as

$$f^D_{g_1} = \frac{L^D_{g_1}}{L_{g_1}}, \tag{3.1}$$

where $L^D_{g_1}$ counts hyperedges with defectors in g_1, a lower $f^D_{g_1}$ indicates higher levels of cooperative clustering and better hyperedge quality within g_1.

To investigate how asymmetric sensitivities affect agents' cooperative behaviours in the system, we use hypergraphs with $g = 3$, fix the synergy factor of low-value games at $r_2 = 0.8$ and set $\delta = 0.06$ and $\delta = 0.09$. In figure 5, we illustrate the variations of various indicators with the two sensitivity factors under both cooperative positive feedback and cooperation collapse scenarios.

When $\delta = 0.09$, figure 5*d* shows that players' average payoff undergoes a significant increase with the rise of the two sensitivities. That is, cooperative behaviour can result in a payoff advantage, and a cooperation-supporting feedback is formed. Figure 5*a* shows an asymmetry in how α_1 and α_2 affect cooperation frequency: high-value regions in the heatmap are concentrated in the right-hand half. This feature is more pronounced in figure 5*b*,*c*. Notably, when $\alpha_2 = 0$, the scale of high-value games remains large, but the quality of hyperedges in g_1 is low; this is because when $\alpha_2 = 0$, all hyperedges in g_2 transition to high-value games with a probability of 1 in the next step, granting g_1 an absolute advantage in scale while significantly reducing the quality of its hyperedges. When $\alpha_2 \neq 0$, unfiltered transitions of hyperedges from g_2 to g_1—which would degrade hyperedge quality—are avoided. On this basis, a higher α_1 ensures the prompt elimination of defectors in g_1, thereby concentrating high-value regions in the right-hand half.

When $\delta = 0.06$, the asymmetric inhibitory effect of sensitivity differences on cooperation is also observed in figure 5*e*. From figure 5*h*, it can be seen that g_1 fails to maintain cooperators' payoff advantage at this point, with low-value regions concentrated in the right-hand half. Although increased sensitivity effectively reduces the proportion of hyperedges containing defectors in g_1 and improves system quality, figure 5*g* shows that hyperedges containing defectors account for approximately 91% of all hyperedges in g_1. Increased α_1 results in extensive filtering of such hyperedges. In addition, g_2 itself has a weak cooperative foundation, and increased α_2 significantly hinders transitions into g_1, leading to continuous shrinkage of g_1's scale. As shown in figure 5*f*, g_2—which cannot sustain cooperation independently—dominates the system, leading to the collapse of cooperation; this further indicates that the imbalance between hyperedge quality and scale, caused by g_1's failure to maintain cooperators' payoff advantages, is the key reason for cooperation failure in state-dependent transitions.

Analysis of the two core cooperative dynamics—positive feedback and cooperation collapse—reveals that the two sensitivity parameters control how easily hyperedges switch to the high-value game g_1, directly shape key cooperative outcomes, and play distinct roles in regulating g_1's quality and scale: for quality control, α_1 filters out low-quality hyperedges to maintain the cooperative purity of original g_1 hyperedges while α_2 ensures hyperedges transitioning from g_2 to g_1 meet quality standards and prevents unregulated quality decline; for scale control, α_1 limits the number of hyperedges leaving g_1 by weeding out low-quality ones whereas α_2 governs the number of hyperedges switching from g_2 to g_1. While higher defection sensitivity improves g_1 hyperedge quality ($f_{g_1}^D$), this alone cannot generate cooperative positive feedback—the scale of g_1 (f_{g_1}) is equally critical, as positive feedback only forms when g_1's quality and scale improve in tandem; imbalances between these two indicators will cause continuous declines in f_{g_1} and eventually lead to cooperation collapse.

4. Conclusion

In this study, we propose and investigate a PGG model by using game transition mechanisms based on URH, aimed at addressing the limitation of traditional pairwise interaction systems in capturing complex dynamics between individual strategies and group environments, and revealing the coevolution of individual strategies and group game states in collective interactions.

We examine the coevolution of strategy selection and game state transitions in PGG on URH. The analysis of state-independent transitions reveals three characteristic cooperation patterns that emerge as the sensitivity parameter α increases: positive feedback, stable cooperation and collapse of cooperation. The evolutionary outcome depends on the respective cooperation levels of the two game states. Extending the model to state-dependent transitions demonstrates asymmetric effects of the sensitivity parameters. Furthermore, we explain that the collapse of cooperation stems from an imbalance between the quality and scale of the high-value game system, which is driven by the system's failure to sustain the payoff advantage of cooperation.

Future studies can address the limitations of the proposed model in three directions. First, developing a theoretical framework to analyse the evolutionary dynamics of higher-order and pairwise interactions is a valuable research direction. It will also help reveal the coevolution mechanisms between strategies and the environment from a theoretical perspective. Second, we can incorporate agents' anticipatory behaviours toward game states; this allows individuals to predict the environmental consequences of their strategies and extend myopic decisions to forward-looking ones. The reinforcement learning framework introduced by Pi *et al*. [45] can provide methodological support for this extension. Third, environmental states in the real world often exhibit historical dependence. Future states may not be determined solely by the current state. Introducing memory effects in state transitions, as well as delayed or asynchronous switching, can more realistically characterize the coevolution between individual behaviours and the environment.

Ethics. This work did not require ethical approval from a human subject or animal welfare committee.

Data accessibility. No experimental data were used in this work. The core simulation code for reproducing the results in this paper is openly available in the GitHub repository at https://github.com/Nan2332/Code_for_Cooperation_in_Public_Goods_Games_over_Uniform_Random_Hypergraphs_with_Game_Transitions, and permanently archived on Zenodo [46].

Supplementary material is available online [47].

Declaration of AI use. We have not used AI-assisted technologies in creating this article.

Authors' contributions. N.W.: formal analysis, investigation, methodology, writing—original draft, writing—review and editing; X.X.: formal analysis, investigation, methodology, writing—original draft; Q.L.: conceptualization, formal analysis, project administration, supervision, validation, writing—review and editing; M.F.: conceptualization, funding acquisition, methodology, supervision, writing—original draft, writing—review and editing; A.S.: conceptualization, formal analysis, funding acquisition, writing—review and editing.

All authors gave final approval for publication and agreed to be held accountable for the work performed therein.

Conflict of interest declaration. We declare we have no competing interests.

Funding. This work is supported by the Chongqing Social Science Planning Project under grant no. 2025NDQN41, Natural Science Foundation of Chongqing under grant no. CSTB2025YITP-QCRCX0007, and National Research, Development and Innovation Office (NKFIH) under grant no. K142948.

Acknowledgements. We thank the editors and reviewers for their advice and dedicated efforts.

References

1. Nowak MA, Highfield R. 2011 *SuperCooperators: altruism, evolution, and why we need each other to succeed*. New York, NY: Free Press.
2. Rand DG, Nowak MA. 2013 Human cooperation. *Trends Cogn. Sci.* **17**, 413–425. (doi:10.1016/j.tics.2013.06.003)
3. Dawes RM. 1980 Social dilemmas. *Annu. Rev. Psychol.* **31**, 169–193. (doi:10.1146/annurev.ps.31.020180.001125)
4. Nowak MA. 2006 Five rules for the evolution of cooperation. *Science* **314**, 1560–1563. (doi:10.1126/science.1133755)
5. Yue H, Xiong X, Feng M, Szolnoki A. 2025 Coevolution of relationship-driven cooperation under recommendation protocol on multiplex networks. *Chaos Solitons Fract.* **190**, 115753. (doi:10.1016/j.chaos.2024.115753)
6. Zeng Z, Feng M, Liu P, Kurths J. 2025 Complex network modeling with power-law activating patterns and its evolutionary dynamics. *IEEE Trans. Syst. Man Cybern. Syst.* **55**, 2546–2559. (doi:10.1109/TSMC.2025.3525465)
7. Feng M, Zeng Z, Li Q, Perc M, Kurths J. 2024 Information dynamics in evolving networks based on the birth-death process: random drift and natural selection perspective. *IEEE Trans. Syst. Man Cybern. Syst* **54**, 5123–5136. (doi:10.1109/TSMC.2024.3389095)
8. Zeng Z, Feng M, Perc M, Kurths J. 2025 Bursty switching dynamics promotes the collapse of network topologies. *Proc. R. Soc. A* **481**, 20240936. (doi:10.1098/rspa.2024.0936)

9. Pi B, Feng M, Deng LJ. 2024 A memory-based spatial evolutionary game with the dynamic interaction between learners and profiteers. *Chaos Interdiscip. J. Nonlinear Sci.* **34**, 063120. (doi:10.1063/5.0215761)
10. Zeng Z, Li Q, Feng M. 2022 Spatial evolution of cooperation with variable payoffs. *Chaos Interdiscip. J. Nonlinear Sci.* **32**, 073118. (doi:10.1063/5.0099444)
11. Szolnoki A, Perc M. 2016 Competition of tolerant strategies in the spatial public goods game. *New J. Phys.* **18**, 083021. (doi:10.1088/1367-2630/18/8/083021)
12. Zhang G, Yao Y, Zeng Z, Feng M, Chica M. 2025 The evolution of cooperation in spatial public goods game with tolerant punishment based on reputation threshold. *Chaos Interdiscip. J. Nonlinear Sci.* **35**, 013104. (doi:10.1063/5.0250120)
13. Hardin G. 1968 The tragedy of the commons. *Science* **162**, 1243–1248. (doi:10.1126/science.162.3859.1243)
14. Milinski M, Semmann D, Krambeck HJ. 2002 Reputation helps solve the 'tragedy of the commons'. *Nature* **415**, 424–426. (doi:10.1038/415424a)
15. Kraak SB. 2011 Exploring the 'public goods game' model to overcome the tragedy of the commons in fisheries management. *Fish Fish.* **12**, 18–33. (doi:10.1111/j.1467-2979.2010.00372.x)
16. Szolnoki A, Perc M. 2010 Reward and cooperation in the spatial public goods game. *Europhys. Lett.* **92**, 38003. (doi:10.1209/0295-5075/92/38003)
17. Helbing D, Szolnoki A, Perc M, Szabó G. 2010 Defector-accelerated cooperativeness and punishment in public goods games with mutations. *Phys. Rev. E* **81**, 057104. (doi:10.1103/PhysRevE.81.057104)
18. Perc M, Szolnoki A. 2008 Social diversity and promotion of cooperation in the spatial Prisoner's dilemma game. *Phys. Rev. E* **77**, 011904. (doi:10.1103/PhysRevE.77.011904)
19. Santos FC, Santos MD, Pacheco JM. 2008 Social diversity promotes the emergence of cooperation in public goods games. *Nature* **454**, 213–216. (doi:10.1038/nature06940)
20. He S, Li Q, Feng M, Szolnoki A. 2026 Reputation assimilation mechanism for sustaining cooperation. *Chaos Solitons Fract.* **202**, 117586. (doi:10.1016/j.chaos.2025.117586)
21. Li A, Wu T, Cong R, Wang L. 2013 One step memory of group reputation is optimal to promote cooperation in public goods games. *Europhys. Lett.* **103**, 30007. (doi:10.1209/0295-5075/103/30007)
22. Xu Z, Li R, Zhang L. 2019 The role of memory in human strategy updating in optional public goods game. *Chaos Interdiscip. J. Nonlinear Sci.* **29**, 043128. (doi:10.1063/1.5081935)
23. Huang C, Wang C. 2024 Memory-based involution dilemma on square lattices. *Chaos Solitons Fract.* **178**, 114384. (doi:10.1016/j.chaos.2023.114384)
24. Szolnoki A, Perc M, Szabó G, Stark HU. 2009 Impact of aging on the evolution of cooperation in the spatial Prisoner's dilemma game. *Phys. Rev. E* **80**, 021901. (doi:10.1103/PhysRevE.80.021901)
25. Perc M, G'omez-Garde nes J, Szolnoki A, Flor'ia LM, Moreno Y. 2013 Evolutionary dynamics of group interactions on structured populations: a review. *J. R. Soc. Interface* **10**, 20120997. (doi:10.1098/rsif.2012.0997)
26. Alvarez-Rodriguez U, Battiston F, de Arruda GF, Moreno Y, Perc M, Latora V. 2021 Evolutionary dynamics of higher-order interactions in social networks. *Nat. Hum. Behav.* **5**, 586–595. (doi:10.1038/s41562-020-01024-1)
27. Hauert C, Saade C, McAvoy A. 2019 Asymmetric evolutionary games with environmental feedback. *J. Theor. Biol.* **462**, 347–360. (doi:10.1016/j.jtbi.2018.11.019)
28. Ito H, Yamamichi M. 2024 A complete classification of evolutionary games with environmental feedback. *PNAS Nexus* **3**(11), 455. (doi:10.1093/pnasnexus/pgae455)
29. Tilman AR, Plotkin JB, Akçay E. 2020 Evolutionary games with environmental feedbacks. *Nat. Commun.* **11**, 915. (doi:10.1038/s41467-020-14531-6)
30. Hilbe C, Šimsa Š, Chatterjee K, Nowak MA. 2018 Evolution of cooperation in stochastic games. *Nature* **559**, 246–249. (doi:10.1038/s41586-018-0277-x)
31. Su Q, McAvoy A, Wang L, Nowak MA. 2019 Evolutionary dynamics with game transitions. *Proc. Natl. Acad. Sci. USA* **116**, 25398–25404. (doi:10.1073/pnas.1908936116)
32. Feng M, Pi B, Deng LJ, Kurths J. 2024 An Evolutionary game with the game transitions based on the Markov process. *IEEE Trans. Syst. Man Cybern. Syst.* **54**, 609–621. (doi:10.1109/TSMC.2023.3315963)
33. Mayfield MM, Stouffer DB. 2017 Higher-order interactions capture unexplained complexity in diverse communities. *Nat. Ecol. Evol.* **1**, 0062. (doi:10.1038/s41559-016-0062)
34. Battiston F *et al.* 2021 The physics of higher-order interactions in complex systems. *Nat. Phys.* **17**, 1093–1098. (doi:10.1038/s41567-021-01371-4)
35. Zhang Y, Lucas M, Battiston F. 2023 Higher-order interactions shape collective dynamics differently in hypergraphs and simplicial complexes. *Nat. Commun.* **14**, 1605. (doi:10.1038/s41467-023-37190-9)
36. Feng L, Gong H, Zhang S, Wu R. 2024 Hypernetwork modeling and topology of high-order interactions for complex systems. *Proc. Natl. Acad. Sci. USA* **121**, e2412220121. (doi:10.1073/pnas.2412220121)
37. Pan J, Zhang L, Han W, Huang C. 2023 Heterogeneous investment promotes cooperation in spatial public goods game on hypergraphs. *Physica A Stat. Mech. Appl.* **609**, 128400. (doi:10.1016/j.physa.2022.128400)
38. Zou K, Han W, Zhang L, Huang C. 2024 The spatial public goods game on hypergraphs with heterogeneous investment. *Appl. Math. Comput.* **466**, 128450. (doi:10.1016/j.amc.2023.128450)
39. Civilini A, Sadekar O, Battiston F, Gómez-Gardeñes J, Latora V. 2024 Explosive cooperation in social dilemmas on higher-order networks. *Phys. Rev. Lett.* **132**, 167401. (doi:10.1103/PhysRevLett.132.167401)
40. Battiston F, Capraro V, Karimi F, Lehmann S, Migliano AB, Sadekar O, Sánchez A, Perc M. 2025 Higher-order interactions shape collective human behaviour. *Nat. Hum. Behav.* **9**, 2441–2457. (doi:10.1038/s41562-025-02373-5)
41. Shi J, Liu C, Liu J. 2024 Hypergraph-based model for modeling multi-agent Q-learning dynamics in public goods games. *IEEE Trans. Netw. Sci. Eng.* **11**, 6169–6179. (doi:10.1109/TNSE.2024.3473941)
42. Zou K, Huang C. 2026 Cooperation dynamics on hypergraphs with punishment and Q-learning. *Expert Syst. Appl.s* **296**, 128989. (doi:10.1016/j.eswa.2025.128989)
43. Ren T, Yao X, Li Y, Zeng XJ. 2025 Bottom-up reputation promotes cooperation with multi-agent reinforcement learning. In *Proc. of the 24th Int. Conf. on Autonomous Agents and Multiagent Systems*, pp. 1745–1754. Richland, SC: IFAAMAS. (doi:10.65109/FDXO1013)
44. Han TA, Song Z, Cimpeanu T, Duong MH, Krellner M, Capraro V, Perc M. 2026 Cooperation versus social welfare. *Phys. Life Rev.* **56**, 33–60. (doi:10.1016/j.plrev.2025.11.006)
45. Pi B, Deng LJ, Feng M, Perc M, Kurths J. 2025 Dynamic evolution of complex networks: a reinforcement learning approach applying evolutionary games to community structure. *IEEE Trans. Pattern Anal. Mach. Intell.* **47**, 8563–8582. (doi:10.1109/TPAMI.2025.3579895)
46. Wei N, Xiong X, Li Q, Feng M, Szolnoki A. 2025 Cooperation in public goods games over uniform random hypergraphs with game transitions. Zenodo repository. (doi:10.5281/zenodo.19371118)
47. Wei N, Xiong X, Li Q, Feng M, Szolnoki A. 2026 Supplementary material from: Cooperation in public goods games over uniform random hypergraphs with game transitions. Figshare. (doi:10.6084/m9.figshare.c.8439809)

Supplementary Material for Cooperation in Public Goods Games over Uniform Random Hypergraphs with Game Transitions

Nankun Wei, Xiaojin Xiong, Qin Li, Minyu Feng, Attila Szolnoki

Journal of the Royal Society Interface

DOI: 10.1098/rsif.2025.1319

S1 Comparison between Pairwise Networks and URH

This section intuitively illustrates the distinct group definitions of higher-order networks and pairwise networks in Fig. S1. Taking the network in Part I of Fig. S1 as an example, Parts II and III describe the interaction groups of player a based on the group definition of higher-order networks and the traditional pairwise network definition (where groups are constructed as a central player plus its neighbors), respectively. The results clearly demonstrate that the group definition in higher-order networks is rigorous and concise, whereas the ambiguous group definition in pairwise networks leads to two critical issues: distorted interactions caused by including non-directly connected players in the same group, and repeated games arising from group membership changes when the central player shifts. These observations highlight the significant advantage of higher-order networks as a more suitable spatial structure for modeling group interactions.

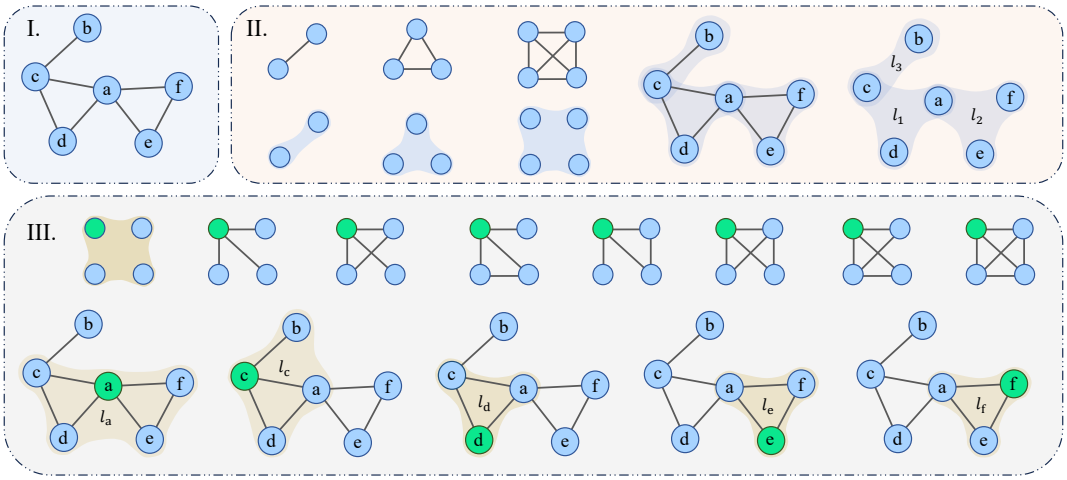

Figure S1: **Comparison of group definitions between higher-order networks and pairwise networks.** Part I shows a pairwise network. We then describe the groups containing agent a using different definitions: Part II illustrates the hypergraph group definition, where each hyperedge corresponds to a complete pairwise subgraph of equal size, and presents the group structure of the network in Part I under this definition—here, player a belongs only to groups l_1 and l_2. Part III takes 4-player groups as an example to demonstrate that the pairwise network's indirect group definition (central player plus neighbors) homogenizes seven distinct pairwise structures into a single group type. Applying this definition to player a reveals membership in $4+1$ groups: group l_a with a as the center, and four additional groups centered at neighbors c, d, e, and f, respectively. The ambiguous group definition leads to two key problems: 1. Group l_c (centered at c) includes non-interacting players a and b, improperly expanding the scope of strategy diffusion and causing their behaviors to mutually influence each other's payoffs in the context of game transitions; 2. Players a, f, and e are repeatedly included in nominally distinct groups l_e and l_f due to central player shifts, resulting in redundant interactions.

While pairwise networks lack clear group definitions and are thus unsuitable for hosting higher-order

interactions, they are naturally compatible with pairwise interactions. In the simulations shown in Fig 2 of the main text, we compared the cooperative dynamics of pairwise interactions ($g = 2$) and higher-order interactions ($g > 2$) on URH. It is therefore necessary to verify whether pairwise interactions characterized by URH differ significantly from those modeled by traditional pairwise networks.

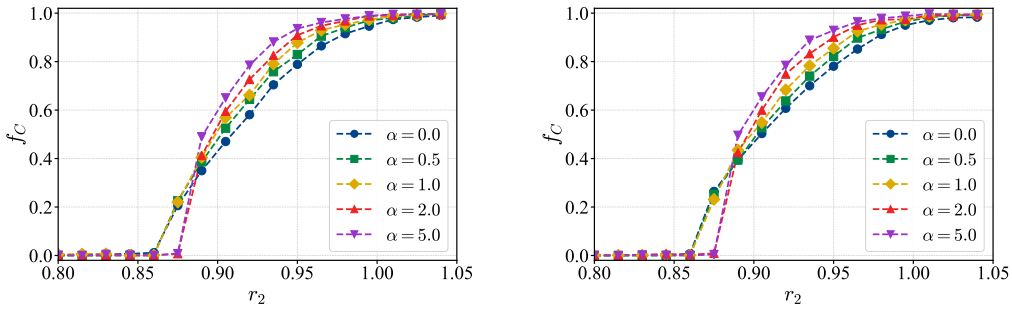

(a) ER random graph (b) URH ($g = 2$)

Figure S2: **Comparison of cooperation dynamics between ER random graphs and URH.** Both networks are configured with $|N| = 1000$ and $\delta = 0.05$. The average degree $\bar{k}$ of the ER random graph is set according to Eq. S1. The same legend symbols represent identical α values, with specific settings detailed in the legend.

According to the URH construction algorithm, when the hypergraph order $g = 2$, the network degenerates into a random network with a Poisson degree distribution. We thus select the classic pairwise random network, the Erdős–Rényi (ER) random graph, for comparison. It should be noted that while both networks follow a Poisson degree distribution, they are not strictly identical. To eliminate potential confounding effects from slight differences in degree distributions on cooperative dynamics, we set the same network size for both structures. The average degree $\bar{k}$ of the ER random graph is defined as:

$$\bar{k} = \left\lfloor \frac{L_c \cdot g}{N} \right\rfloor, \tag{S1}$$

where g denotes the order of URH, and $L_c = (N/g) \ln N$ represents the minimum number of hyperedges required to maintain URH connectivity.

We set $|N| = 1000$ and $\delta = 0.05$, and investigate whether the impact of different sensitivity parameters on cooperation frequency exhibits consistency across the two networks as r_2 increases. The simulation results are presented in Fig. S2, which shows that as r_2 grows, the effect of high sensitivity on cooperation frequency transitions from inhibition to promotion in both networks. The nearly identical cooperative dynamics confirm that URH can effectively model pairwise interactions when $g = 2$.

S2 Robustness Check with Different Initial Conditions

The simulations presented in the main text, the strategies of agents, and the game states of hyperedges were randomly initialized with a 50% probability for each type. Specifically, cooperators and defectors each accounted for 50% of the population, and hyperedges in the two game states also each constituted 50% of the total. Considering that initial conditions may induce path dependence or bistability, we verify the numerical stability of the research results by adopting different initialization ratios for the initial strategies of nodes and the initial game states of hyperedges on the Uniform Random Hypergraph (URH). Under different parameter configurations, we plotted the evolutionary time-series curves of cooperation frequency f_C. The results demonstrate that different initialization ratios only affect the evolutionary trends of f_C before convergence, but do not alter its final steady-state mean value. The detailed simulation setup and analysis are provided below.

For clarity of exposition, we define the initial proportion of cooperators (C) as $f_C^{T=0}$, and the initial proportion of defectors (D) is accordingly $f_D^{T=0} = 1 - f_C^{T=0}$. Similarly, the initial proportion of

hyperedges in the high-value game state (g_1) is denoted as $f_{g_1}^{T=0}$, and the proportion of hyperedges in the low-value game state (g_2) is $f_{g_2}^{T=0} = 1 - f_{g_1}^{T=0}$.

As shown in Fig S3, each subplot contains four scatter curves corresponding to $f_C^{T=0}$ ranges from 0.2 to 0.8 in steps of 0.2, respectively. Columns 1 to 3 represent $f_{g_1}^{T=0} = 0.1$, 0.5, and 0.9, respectively. For the other model parameters, the relative resource advantage of the high-value game $\delta = 0.05$ is fixed, and three combinations of α and r_2 are adopted. The first row corresponds to $\alpha = 0$ and $r_2 = 0.82$; the second row corresponds to $\alpha = 1$ and $r_2 = 0.85$; the third row corresponds to $\alpha = 5$ and $r_2 = 0.88$.

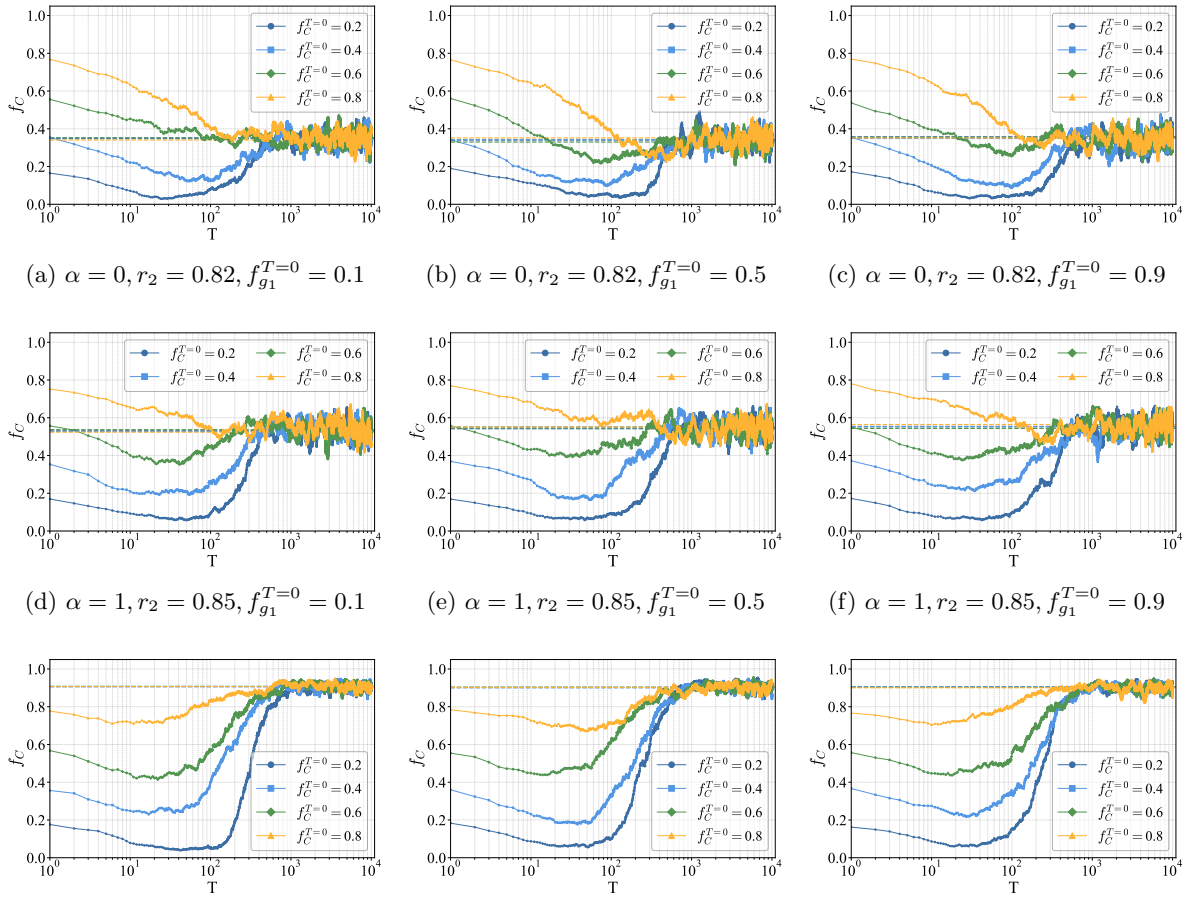

(a) $\alpha = 0, r_2 = 0.82, f_{g_1}^{T=0} = 0.1$ (b) $\alpha = 0, r_2 = 0.82, f_{g_1}^{T=0} = 0.5$ (c) $\alpha = 0, r_2 = 0.82, f_{g_1}^{T=0} = 0.9$

(d) $\alpha = 1, r_2 = 0.85, f_{g_1}^{T=0} = 0.1$ (e) $\alpha = 1, r_2 = 0.85, f_{g_1}^{T=0} = 0.5$ (f) $\alpha = 1, r_2 = 0.85, f_{g_1}^{T=0} = 0.9$

(g) $\alpha = 5, r_2 = 0.88, f_{g_1}^{T=0} = 0.1$ (h) $\alpha = 5, r_2 = 0.88, f_{g_1}^{T=0} = 0.5$ (i) $\alpha = 5, r_2 = 0.88, f_{g_1}^{T=0} = 0.9$

Figure S3: **Evolutionary time-series of cooperation frequency under different initial conditions.** Each subplot depicts the evolutionary trajectory of f_C over Monte Carlo steps. Four curves are shown in each subplot, corresponding to initial cooperator proportions $f_C^{T=0} = 0.2$ (dark blue), 0.4 (blue), 0.6 (green), and 0.8 (yellow), respectively. Subplots (a)–(c) use $\alpha = 0$ and $r_2 = 0.82$; subplots (d)–(f) use $\alpha = 1$ and $r_2 = 0.85$; subplots (g)–(i) use $\alpha = 5$ and $r_2 = 0.88$. Columns correspond to distinct initial proportions of high-value hyperedges. The first column corresponds to $f_{g_1}^{T=0} = 0.1$, the second column to $f_{g_1}^{T=0} = 0.5$, and the third column to $f_{g_1}^{T=0} = 0.9$. In all cases, $\delta = 0.05$ is fixed.

All subplots in Fig S3 share a common characteristic: while different initial cooperator proportions intuitively influence the evolutionary trajectory of f_C prior to convergence, f_C ultimately converges to the same steady-state range. A horizontal comparison of the subplots within each row shows that variations in the initialization ratio of hyperedge states have no significant impact on evolutionary trends, nor do they alter the steady-state mean of f_C. Vertically, the results confirm that for each set of transition parameters, varying initial cooperator proportions do not hinder the convergence of f_C to the steady-state range specific to that parameter set. Collectively, these findings sufficiently validate the robustness of the numerical results presented in the main text with respect to variations in initialization ratios.

S3 Robustness Check on Mixed-Order Hypergraphs

In the main text, simulations and analyses on URH show that higher-order interactions promote cooperation more effectively than pairwise interactions. Moreover, the transition mechanism leads to a stronger nonlinear response of cooperation frequency to environmental sensitivity under higher-order interactions.

To verify the robustness of these conclusions, we constructed homogeneous mixed-order hypergraphs with random connections. We performed simulations on mixed-order hypergraphs using the same parameters as in Fig. 2(a) and (e) of the main text. Simulation results and conclusions are highly consistent with those from URH analyses. This confirms the robustness of our core conclusions.

S3.1 Construction of mixed-order hypergraphs

In the hypergraph framework, a mixed-order URH is denoted as $H'(N, L)$, where $N = \{n_1, n_2, \ldots, n_n\}$ represents a set of N nodes. $L = \{l_1, l_2, \ldots, l_m\}$ denotes a set of L hyperedges, each corresponding to a group for Public Goods Games.

Unlike pure g-order uniform hypergraphs, mixed-order hypergraphs include hyperedges of multiple different orders. We first define a set of hyperedge orders $\mathcal{G}$. Each order $g \in \mathcal{G}$ is assigned a weight w_g, which determines the exact proportion of hyperedges of order g in the final network. The weights satisfy $\sum_{g\in\mathcal{G}} w_g = 1$. We further define the average hyperedge order $\bar{g}$ as the weighted average of all hyperedge orders in $\mathcal{G}$, to quantify the mean group size of interactions in the mixed-order hypergraph, calculated as:

$$\bar{g} = \sum_{g\in\mathcal{G}} w_g \cdot g. \tag{S2}$$

The total number of hyperedges $L_{\mathcal{G}}$ is determined by the weighted average of critical thresholds across all orders in $\mathcal{G}$:

$$L_W = \sum_{g\in\mathcal{G}} w_g \cdot \frac{N}{g} \ln N, \tag{S3}$$

where $N \cdot \ln N/g$ is the critical hyperedge number L_c for a pure g-order URH. The final $L_{\mathcal{G}}$ is obtained by rounding down L_W and adding 1 to ensure sufficient hyperedges for network connectivity.

We assign the number of hyperedges for each order g according to the predefined weights w_g. Each hyperedge of order g is formed by randomly sampling g distinct nodes with no repeated nodes within a single hyperedge, and each agent may belong to multiple hyperedges simultaneously. After generating all hyperedges, we perform a final check to ensure the connectivity of the resulting hypergraph.

S3.2 Simulations on randomly connected mixed-order hypergraphs

To ensure comparability with the main text setup, we define the hyperedge order set $\mathcal{G} = \{2, 3, 4, 5\}$, which is fully consistent with the order selection in the main text. We adopt four weight distributions of hyperedge orders as listed in Table S1. For each distribution, we compute the corresponding average order $\bar{g}$, which is further used to calculate the normalized synergy factor. We performed simulations on hypergraphs generated from these four distributions using the same parameters as in Fig. 2(a) and Fig. 2(e) of the main text, and the detailed results are displayed in Fig. S4.

Table S1: Hyperedge weight distributions and corresponding average order $\bar{g}$.

Distribution	$w_{g=2}$	$w_{g=3}$	$w_{g=4}$	$w_{g=5}$	$\bar{g}$
1	0.70	0.15	0.05	0.10	2.55
2	0.35	0.40	0.15	0.10	3.00
3	0.20	0.25	0.30	0.25	3.6
4	0.05	0.15	0.40	0.40	4.15

Results confirm that higher average hyperedge orders still promote cooperation more effectively than pairwise interactions. In Fig. S4, compared to Panel (a), Panel (b) introduces game transitions

with strong environmental sensitivity $\alpha = 5$. As r_2 increases, the intensity of social dilemmas in low-value games g_2 diminishes, leading to a distinct nonlinear trend in f_C where cooperation is suppressed at low r_2 but strongly promoted at high r_2. This nonlinear trend becomes more prominent for hypergraphs with higher average orders $\bar{g}$. This shows that environmental sensitivity still has a strong nonlinear effect on f_C in mixed-order structures. The effect grows stronger with increasing average hyperedge order $\bar{g}$. These findings agree with those from pure g-order URH.

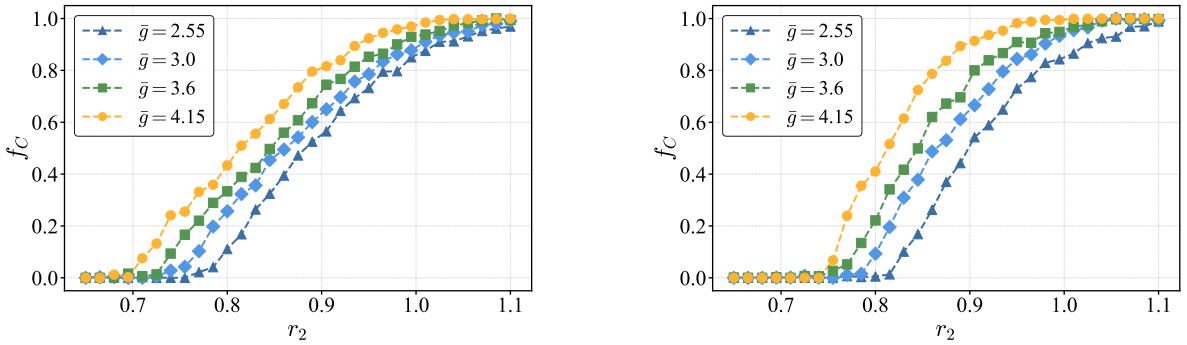

(a) $\alpha = 0.00, \delta = 0.05$ (b) $\alpha = 5.00, \delta = 0.05$

Figure S4: **Cooperation frequency f_C as a function of r_2 on mixed-order hypergraphs.** The x-axis represents the low-value synergy factor r_2, with curves for four weight distributions of hyperedge orders (Table S1) characterized by different average hyperedge orders $\bar{g}$. Panels (a) and (b) set $\delta = 0.05$ with $\alpha = 0$ and 5, respectively.